Morphology-dependent thermoelectric properties of mixed phases of copper sulfide (Cu$_{2-x}$S) nanostructures synthesized by hydrothermal method

Yahya Muddassir[1] · Sofia Tahir[1,2] · Adnan Ali[1] · Khalid Mahmood[1] · Ubaid Ur Rehman[1] · Arslan Ashfaq[1] · Alina Manzoor[1] · Salma Ikram[1]

Abstract

In this research work we have synthesized copper sulfide (Cu$_{2-x}$S) nanostructures by the hydrothermal method. The post-sulfurization was performed by using tube furnace to reduce sulfur deficiency and to minimize impurities present in the crystal-lattice. The samples were synthesized by various pH values of precursor solution. The samples were characterized by XRD, RAMAN spectroscopy, SEM, Hall measurements and Seebeck effect. XRD analysis revealed the formation of hexagonal covellite (CuS) and chalcocite (Cu$_2$S) phases of copper sulfide. Despite these phases XRD data also showed the dominating hexagonal digenite (Cu$_{1.8}$S) phase of copper sulfide. We observed a decreasing trend in average crystalline size with the increasing pH values of the samples from the XRD data. We have found maximum average crystalline size of 39.1679 nm at pH value of 4. The formation of LO mode of hexagonal covellite phase of copper sulfide was observed from RAMAN analysis. The SEM images revealed the formation of flower-like nanostructures at the lowest pH value. It strengthened our argument that the crystallinity of nanostructures is inversely proportional to the pH value. We have achieved maximum values of Seebeck coefficient and conductivity at room temperature as 73.920 µV/K and 0.909 S/cm, respectively. The Seebeck coefficient and conductivity graphs showed an increasing trend due to the energy filtering effect in mesoporous structure. The maximum value of power factor was 4.91×10^{-7} Wm^{-1} K^{-2}.

Keywords Copper sulfide nanostructures · Hexagonal covellite · X-ray diffraction · RAMAN spectroscopy · SEM · Power factor

1 Introduction

In the world of nanotechnology, chalcogenides is a most active researched group among all the semiconductors due to an interesting phenomenon of quantum confinement effect. Copper sulfide is considered as a good thermoelectric material. Good thermoelectric materials are cheap, environmentally friendly, and alternative to power generators. Research on thermoelectric properties has steadily been increased in the middle of 90th century. Synthesis of high temperature resistant thermoelectric materials is an active research field.

A wide class of materials having revolutionary and cost-efficient applications have been studied and their properties have been improved [1, 2]. Thermoelectric materials became an active research site for the researchers due to their tunable thermoelectric properties. The working of thermoelectric materials depends on three basic laws of thermoelectricity of Seebeck effect, Peltier effect and Thomson effect) [3]. In 1957, Loffe proposed a mathematical relation to calculate the exact value of figure of merit of thermoelectric material. Materials having low thermal conductivity and high power factor are considered as good thermoelectric materials [2].

Copper sulfide has wide range of applications and can be stabilized in various valance configurations of chalcocite (Cu$_2$S), digenite (Cu$_9$S$_5$), anilite (Cu$_7$S$_4$), djurleite (Cu$_{1.95}$S), covellite (CuS) and hexagonal digenite (Cu$_{1.8}$S) phases. Copper sulfide is visible light active semiconductor due to the presence of narrow band gap of (1.2–2.3) eV and can be used in various applications. Active research areas in the

✉ Sofia Tahir
  sofetahir@gmail.com

1   Government College University Faisalabad, Faisalabad 38000, Pakistan

2   University of New South Wales, Sydney, Australia

world of copper sulfide are uses of copper sulfide as pollutant treatment, degradation of methylene blue, artificial photosynthesis, photocatalysis in the presence of white light, etc. CuS nanotubes also showed a very good oxidation and reduction capabilities toward methylene blue. Degradation of Rhodamine B (Rh B) can be done easily up to 99.7% by using mixed phases of copper sulfide nanoparticles (CuS-Cu_7S_4). Snowflake-like copper sulfide (Cu_2S) structures are used for light trapping and scattering because of its high surface area. Copper sulfide is very good p-type semiconductor material and has unique optical and electronic properties [1, 4].

Copper sulfide nanostructures can be synthesized by several methods, such as hydrothermal, ball milling, high temperature injection route, colloidal solution method, pulsed plasma-assisted route, direct synthesis from precursors, ion exchange method, etc. However, the hydrothermal route is the easiest and cost-effective method for the synthesis of pure copper sulfide nanostructures [1, 5, 6].

Tang et al., synthesized copper sulfide (Cu_2S) microcrystals and nanocrystals by using hydrothermal and wet chemistry routes, respectively. They synthesized copper sulfide nanoparticles having size of (1–7) μm by using hydrothermal method. They concluded that internal arrangement of atoms and phase structures highly depends upon reaction temperature and time [7]. Zhang et al., synthesized copper sulfide nanoparticles by using hydrothermal technique for the first time. In which they used CH_4N_2S as a source of sulfur and $C_2H_8N_2$ (Ethylenediamine) as a solvent. They observed that Cu_2S snowflake samples showed higher photovoltaic activity than rest of samples [8].

Li et al., synthesized nanowires of roxbyite phase of copper sulfide Cu_7S_4 on two different substrates of silicon Si, and indium tin oxide. They reported that nanowires on Si-coated glass substrate have both orthorhombic and monoclinic phases, while on ITO-coated glass substrate has only monoclinic phase [9]. Chen et al., regarded Cu_2S as a good thermoelectric material. They synthesized $Cu_{2-x}S$ with scalable wet chemical technique. Using high temperature annealing techniques, they changed the morphology of synthesized nanoparticles from orthorhombic to tetragonal. They observed that the maximum value of figure of merit is 1.04 at 773 K due to phonon scattering and formation of interface of $Cu_{2-x}S$ [10].

Shaikh et al., reported that metal chalcogenides like copper sulfide show advanced performance in the field of super capacitor because of their good electrochemical properties [11].

The improvement in thermoelectric properties of copper sulfide nanostructures can be done with high figure of merit. It can only be possible for having high electrical but low thermal conductivity. This is not an easy task as both quantities are directly proportional to each other.

To control electrical and thermal conductivity, researchers introduce nanowire nanostructures and super lattice structure approaches [12]. Copper sulfide shows an energy filtering effect due to the unique mesoporous crystal structure. Mesoporous structure provides short ion/electron diffusion path and more active sites for electrochemical reaction. Recently, mesoporous structures of copper sulfide were synthesized by microwave irradiation route and used in super capacitors [13]. Thermoelectric properties were improved by post-sulfurization of the prepared nanostructures [14].

In this research work, we have synthesized mixed phases of copper sulfide ($Cu_{2-x}S$) nanostructures by the hydrothermal method. Then the samples were sulfurized to remove the sulfur deficiency from copper sulfide crystal-lattice. We have performed different characterization techniques of XRD, RAMAN and SEM to check the structural and thermoelectric properties of copper sulfide nanostructures with increasing pH values and the formation of mesoporous structure. The literature survey showed that no research work has yet been reported on the morphology-dependent thermoelectric properties of copper sulfide nanostructures with different pH values.

2 Experimental section

Copper acetate monohydrate, thiourea, citric acid monohydrate, ethanol and sodium hydroxide were purchased from Sigma and Merck with 99% purity and used without further purification. All copper sulfide samples were prepared by using a simple hydrothermal method. In this typical synthesis we used ethanol as solvent. First, we made solution of copper acetate by adding 3.194 g of $C_4H_8CuO_5 \cdot H_2O$ in 80 ml of ethanol, while constant stirring of $C_4H_8CuO_5 \cdot H_2O$ solution, we have added 6.72 g of citric acid. Such that the blue color of copper acetate solution suddenly turns into light blue. In a second step, we made thiourea solution by adding 3.653 g of CH_4N_2S in 80 ml of ethanol, while stirring of copper acetate and citric acid solution, we added thiourea solution drop by drop. Then, the light blue color of copper acetate and citric acid solution gradually turns into green. Finally, a white slurry solution was obtained. After 15 min of constant stirring, we added NaOH solution to obtain required pH values of 4, 6 and 12. After that, we pour precursor solution into Teflon autoclave and put the autoclave in an oven. The temperature was maintained at 180 °C for 10 h. After cooling down, black colored nanoparticles were collected. They were washed thoroughly with distilled water and then with ethanol. They were dried at 100 °C for 10 h. Finally, black colored copper sulfide nanostructures were sulfurized in a tube furnace at 500 °C for 30 min.

The electrical conductivity and Seebeck coefficient were measured by Hall system (Ecopia 3000) and Seebeck
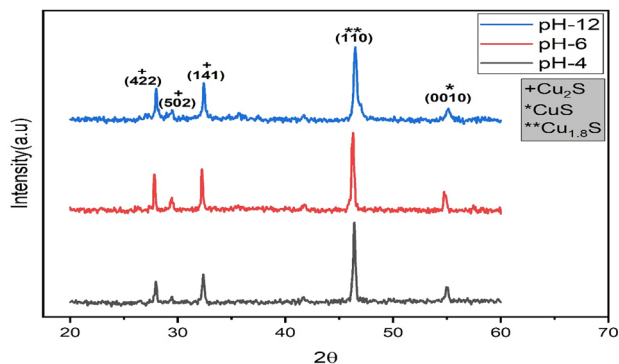
systems (Homemade Seebeck method), respectively. For the verification of secondary phases in copper sulfide nanostructures various characterization techniques were used. We have used X-ray diffraction (Bruker D8 ADVANCED), Raman spectroscopy (MN STEX-PRI 100) with a laser wavelength of 632.8 nm and SEM (EmCraft 100 CUBE Series). The detail can also be found in reference [23].

3 Results and discussion

3.1 XRD analysis of copper sulfide nanostructures synthesized at pH values of 4, 6 and 12

For structural information like crystal defects, crystallinity, crystal texture and phase identification of copper sulfide nanostructures, we used a very powerful and nondestructive tool of X-ray diffraction. The copper sulfide nanoparticles were synthesized with varying pH values and the samples were labeled as A_1, A_2, and A_3.

Figure 1 shows the XRD pattern of sample A_1, A_2, A_3 synthesized at pH value of 4, 6 and 12, respectively. The graph showed that XRD peaks are in 2θ range of 20 to 60. The chalcocite phase (Cu_2S) of copper sulfide was observed at two different 2θ values of 27.9° and 32.3°, oriented at ($\overline{4}2\overline{2}$) and ($\overline{1}4\overline{1}$) planes, respectively. In addition to above two primary phases of chalcocite, a secondary phase was also observed at 2θ value of 29.4° oriented at ($\overline{5}$ 02) planes.

Despite, chalcocite (Cu_2S) phase of copper sulfide, the result showed two other phases of copper sulfide. The XRD pattern showed hexagonal digenite ($Cu_{1.8}S$) phase of copper sulfide at 2θ value of 46.3° oriented at (110) planes. It also showed the secondary hexagonal covellite (CuS) phase of copper sulfide at 2θ value of 55° oriented at (0 $\overline{1}$ 0) planes.

We have used the following relations to calculate different structural parameters of as prepared copper sulfide ($Cu_{2-x}S$) nanostructures. Their values are shown in Table 1.

- $d = n\lambda/2\sin\theta$ where λ is the wavelength of incident X-ray
- $D = 0.89\lambda/\beta\mathrm{Cos}\theta$ where β is the full width half maxima (FWHM)
- $\delta = 1/D^2$ where D is the crystalline size
- $\varepsilon_{\mathrm{strain}} = \beta/4\tan\theta$ where Θ is the diffraction peak [15]

3.2 The effect of pH on average crystalline size of copper sulfide nanostructures

The crystalline size of synthesized copper sulfide nanostructures was calculated by using Debye Scherrer equation (Table 2). The mathematical form of Debye Scherrer equation is given below.

$$D = 0.89\lambda/\beta\mathrm{Cos}\theta$$

where

- D is crystalline size
- λ is the wavelength of incident X-rays (1.54 Å)
- β is full width half maxima
- Θ is the diffraction angle

Fig. 1 XRD pattern of samples A_1, A_2, A_3 synthesized at pH value of 4, 6 and 12

Table 2 Effect of pH on Raman shift and intensity

Sample ID	pH	Raman shift (cm^{-1})	Intensity (a.u)
A_1	4	466	127.544
A_2	6	466.67	82.262
A_3	12	468	125.695

Table 1 Calculated structural parameters of as prepared $Cu_{2-x}S$ nanostructure

Sample ID	2θ (deg)	Intensity (a.u)	FWHM (deg)	Dislocation density (d) (nm^{-2})	Inter-planer spacing (d_{hkl}) (A°)	Micro-strain (e)
A_1	46.397	308.852	0.2692	9.29×10^{-4}	3.03×10^{-2}	1.07×10^{-2}
A_2	46.2	317.76	0.2746	9.68×10^{-4}	3.02×10^{-2}	1.10×10^{-3}
A_3	46.4	306.90	0.3354	1.44×10^{-3}	3.03×10^{-2}	1.34×10^{-3}

Figure 2 shows the maximum crystalline size of 39.1679 nm at pH value of 4. We have best crystal structure at pH value of 4. With the increase in pH value, the crystalline size gradually decreases. It means that we are moving toward porosity.

3.3 Raman analysis of copper sulfide nanostructures

We have used a simple and authentic characterization technique of Raman spectroscopy to check the vibrational modes of copper sulfide ($Cu_{2-x}S$) nanostructures. We synthesized a series of three samples with varying pH values of 4, 6 and 12, respectively.

3.3.1 Raman spectroscopic analysis of copper sulfide nanostructures synthesized at pH values of 4, 6 and 12

Figure 3 shows the Raman graph of copper sulfide nanostructures having pH value of 4, 6 and 12. It showed Raman shift in the range 150 to 1000. The result showed maximum peaks at 466 cm^{-1}, 466.67 cm^{-1}, 468 cm^{-1} due to strong S–S bonding. The maximum peaks at 466 cm^{-1}, 466.67 cm^{-1}, 468 cm^{-1} are the indication of very sharp S–S stretching mode of S_2. The peaks at 466 cm^{-1}, 466.67 cm^{-1}, 468 cm^{-1} peak verifies LO (longitudinal optical) mode vibrations of pure hexagonal covellite copper enriched phase of copper sulfide [16].

We also observed slight red Raman peak shift in our data when we compare it with the reported literature. In the literature, the very sharp peak of both covellite (CuS) and chalcocite (Cu_2S) phases of copper sulfide were observed at 470 cm^{-1}. Therefore, from Raman spectroscopy phase identification is very difficult. In Raman analysis formation of sharp peaks is the indication of fine crystallinity [17].
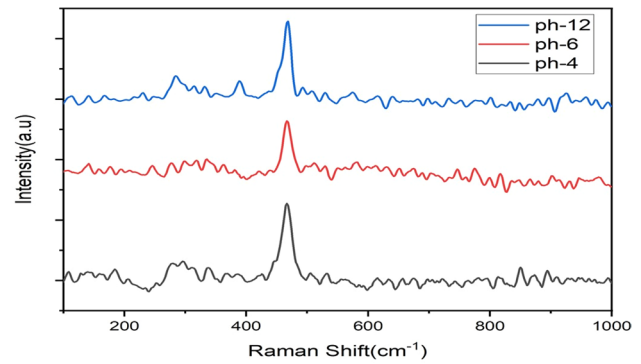
Generally vibrational frequencies that can cause peak shift are controlled by the factors of atomic mass, force constant of lattice atoms and atomic bonds [18].

It is also reported in the literature that the wavelength of Raman signal can also produce peak shift. In our research center, we used Raman beam having wavelength 632.8 nm. This may be the cause of peak shift from the reported data [19].

It is interesting to note that with the increase in pH value, Raman shift gradually moves toward reported value of 468 cm^{-1} which is very close to maximum reported Raman peak shift value for copper sulfide nanostructures. It is commonly assumed that most stable phases of copper sulfide were obtained at higher pH value [17].

3.4 Scanning electron microscopy (SEM) results of copper sulfide nanostructures

In order to observe surface morphology, we used a highly advanced technique of scanning electron microscopy. It is common perception that nanoparticles or nanomaterials showing ordered or best morphology generally exhibit good optical, electrical and thermoelectric properties. Morphology of a nanomaterial can be controlled via various factors:

- Precursors molar ratio
- Reaction time
- pH of the precursor's solution
- Solvents

In this research article we kept all above factors constant and observed the effect of pH on the morphology of copper sulfide nanostructures. We synthesized copper sulfide nanostructures at pH values of 4, 6 and 12 and observed their morphology. Then, we deeply noticed the change in thermoelectric properties with the change in morphology.
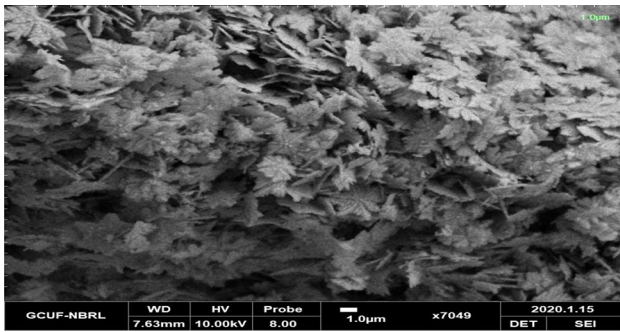
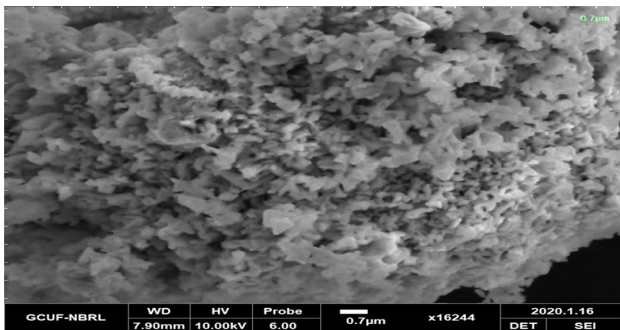**Fig. 4** SEM pattern of sample A_1 synthesized at pH value of 4

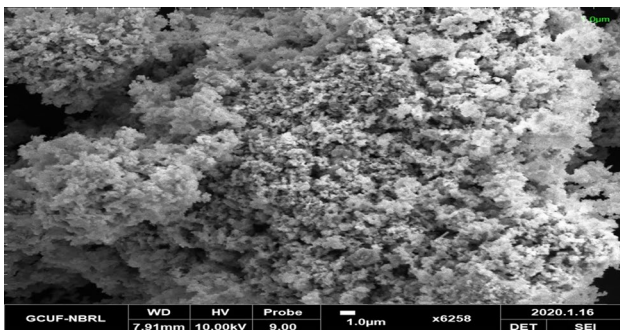**Fig. 5** SEM pattern of sample A_2 synthesized at pH value of 6

Fig. 6 SEM pattern of sample A_3 synthesized at pH value of 12

Figures 4, 5 and 6 shows morphology of copper sulfide nanostructures synthesized at pH value of 4, 6 and 12, respectively. Ideal flower-like morphology was obtained at only moderate pH value of 4. As pH increases, SEM images show that materials move toward porosity. The SEM images at pH value of 6 and 12 shows agglomerated copper sulfide nanostructures [20]. The EDS results of SEM micrographs of copper sulfide nanostructures at different pH values of 4, 6 and 12 are given in Table 3.

Table 3 EDS results of SEM micrograph at different pH values

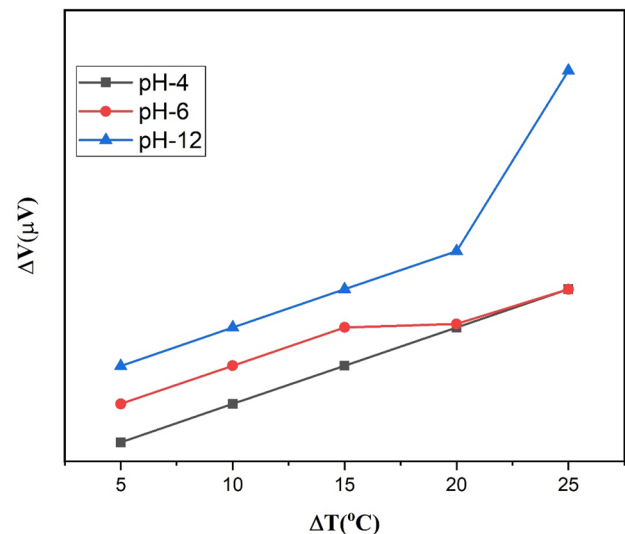| Sample ID	Element	Weight (%)
A_1 (4 pH)	Cu	66.15
	S	33.51
	O	0.34
A_2 (6 pH)	Cu	66.24
	S	33.46
	O	0.30
A_3 (12 pH)	Cu	66.58
	S	33.16
	O	0.26

Fig. 7 Voltage response curve of sample A_1, A_2, A_3 synthesized at pH value of 4, 6 and 12

3.5 Thermoelectric measurements of copper sulfide nanostructures

Figure 7 shows ΔT versus ΔV data of mixed phases of copper sulfide synthesized at pH values of 4, 6 and 12, respectively, under constant heat flow. Data graph plotted between Response Voltage versus constant increasing temperature always showed an increasing trend. It reveals that copper sulfide is a p-type semiconductor.

Figure 8 shows Seebeck coefficient versus pH graph. Seebeck coefficient is basically a positive slope of response voltage versus temperature graph. In the literature maximum reported value of Seebeck coefficient is 80 µV/K at approximately 700 K, but here we achieved its maximum value of 73.920 µV/K at room temperature. We can achieve this at room temperature due to two reasons.

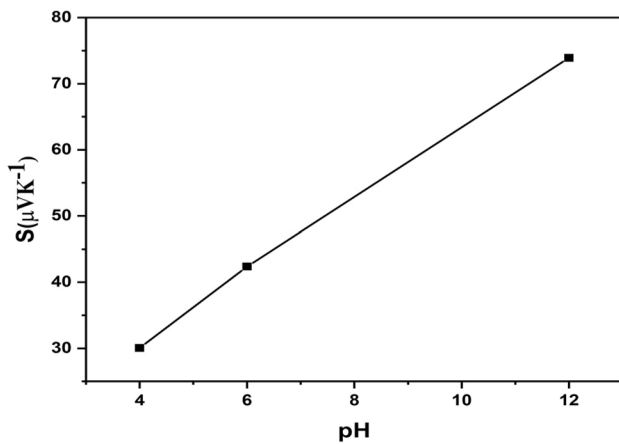**Fig. 8** Seebeck coefficient versus pH graph

- The presence of dominant copper deficient phase $Cu_{1.8}S$ and other similar copper deficient phases which are not detected here due to very small crystalline size.
- Due to very high surface area and very small crystalline size, these pallets of as synthesized mixed phases of copper sulfide gives maximum response voltage. The dimensions of synthesized pallets also contribute in increasing Seebeck coefficient values [21].

Figure 9 shows a clear rise in conductivity of mixed phases of copper sulfide nanostructures calculated by using Hall measurements. We recorded maximum conductivity values of 90.9 S/m or 0.909 S/cm at room temperature.

The conductivity graph shows a constant rise with the increase in the pH value of the precursor solution and the decrease in the crystalline size. That's why the porosity of synthesized nanostructures is increased as shown in the SEM images. The mesoporous structures show an energy filtering effect that allows only high energy carriers to take part in conductivity. Due 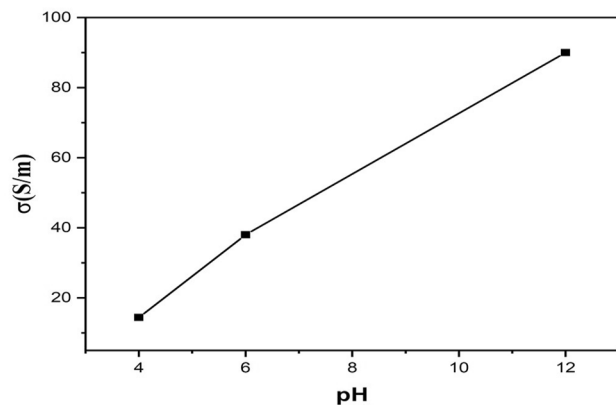to this effect, the electrical conductivity and Seebeck coefficient show an increasing trend. The domination of secondary phases with the rise of pH values contributes to electrical conductivity [22, 23].

Figure 10 shows the effect of copper sulfide nanostructures with varying pH values on the power factor. Since the Seebeck coefficient and conductivity increase with the increase in pH value, the increasing trend of power factor is understandable.

4 Conclusion

In this manuscript we have investigated the effect of morphology on thermoelectric properties of $Cu_{2-x}S$ nanostructures synthesized by the hydrothermal method. From XRD data, we concluded that hexagonal digenite ($Cu_{1.8}S$) phase of copper sulfide is dominating in our synthesized samples. Raman data reveal the formation of LO mode of hexagonal covellite phase of copper sulfide. From XRD and SEM analysis, we concluded that the average crystalline size (nm) of copper sulfide nanostructures is inversely proportional to the pH value of precursor's solution. We have reported the best crystal structure at pH value of 4. We observed that crystalline size gradually decreases with the increase in pH value. It showed that we are moving toward porosity with the increase in pH value of the precursor solution. From thermoelectric measurements (Hall measurements, Seebeck effect), we concluded that the thermoelectric properties of the samples of copper sulfide are directly proportional to the pH value of precursors solution and inversely proportional to the morphology. The results of electrical conductivity and Seebeck effect shows continuous rise. This is due to the energy filtering effect. We have achieved maximum value of power factor (4.91×10^{-7} Wm^{-1} K^{-2}) at pH value of 12 at room temperature.
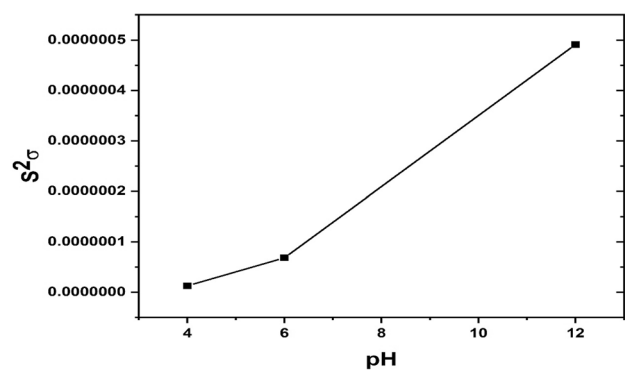

Fig. 9 Conductivity versus pH graph

Fig. 10 Effect of pH value on the power factor

Availability of data and material The data and material is available in this manuscript.

Declarations

Conflict of interest The authors declare that they have no conflict of interest.

Consent to participate Informed consent was obtained from all individual participants included in the study.

Consent for publication The authors would like to give the consent to the publisher to publish this work.

Consent for ethical approval This chapter does not contain any studies with human participants or animals performed by any of the authors.

References

1. Bajpai, P. K., Yadav, S., Tiwari, A., & Virk, H. S. (2015). Recent advances in the synthesis and characterization of chalcogenide nanoparticles. In *Solid State Phenomena* (Vol. 222, pp. 187–233). Trans Tech Publications Ltd
2. Weidenkaff, A. (2017). Thermoelectricity for future sustainable energy technologies. In *EPJ Web of Conferences* (Vol. 148, p. 00010). EDP Sciences
3. A. Bulusu, D.G. Walker, Review of electronic transport models for thermoelectric materials. Superlattices Microstruct. **44**(1), 1–36 (2008)
4. M. Mousavi-Kamazani, M. Salavati-Niasari, M. Ramezani, Preparation and characterization of Cu 2 S nanoparticles via ultrasonic method. J. Cluster Sci. **24**(3), 927–934 (2013)
5. Feng, S. H., & Li, G. H. (2017). Hydrothermal and solvothermal syntheses. In *Modern inorganic synthetic chemistry* (pp. 73–104). Elsevier
6. O. Balayeva, A. Azizov, M. Muradov, Copper sulfide nanomaterials: liquid-phase synthesis. J. Qafqaz Univ. **3**(2), 120–131 (2015)
7. Y.Q. Tang, Z.H. Ge, J. Feng, Synthesis and thermoelectric properties of copper sulfides via solution phase methods and spark plasma sintering. Curr. Comput.-Aided Drug Des. **7**(5), 141 (2017)
8. X. Zhang, Y. Guo, J. Tian, B. Sun, Z. Liang, X. Xu, H. Cui, Controllable growth of MoS2 nanosheets on novel Cu2S snowflakes with high photocatalytic activity. Appl. Catal. B **232**, 355–364 (2018)
9. L. Li, W. Zhang, Synthesis and light absorption properties of copper sulfide nanowire arrays on different substrates. Phys. B **550**, 26–31 (2018)
10. X. Chen, H. Zhang, Y. Zhao, W. Liu, W. Dai, T. Wu, L. Wang, Carbon encapsulated copper sulfide leading to enhanced thermoelectric properties. ACS Appl. Mater. Interfaces **11**(25), 22457–22463 (2019)
11. S. Shaikh, M.K. Rabinal, Rapid ambient growth of copper sulfide microstructures: binder free electrodes for supercapacitor. J. Energy Storage **28**, 101288 (2020)
12. Y. Zhou, Q. Lu, X. Chai, Z. Xu, J. Chen, A. Krier, L. He, InAs/GaSb superlattice interband cascade light emitting diodes with high output power and high wall-plug efficiency. Appl. Phys. Lett. **114**(25), 253507 (2019)
13. M. Naveed, W. Younas, Y. Zhu, S. Rafai, Q. Zhao, M. Tahir, C. Cao, Template free and facile microwave-assisted synthesis method to prepare mesoporous copper sulfide nanosheets for high-performance hybrid supercapacitor. Electrochim. Acta **319**, 49–60 (2019)
14. U. Rehman, J. Jacob, K. Mahmood, A. Ali, A. Ashfaq, M. Basit, N. ur Rehman, Improving the thermoelectric performance of hydrothermally synthesized FeS2 nanoparticles by post sulfurization. Ceram. Int. **46**, 20496–20499 (2020)
15. Z.J. Shanan, Synthesis and characterization of CuS/PVA nanocomposite via chemical method. IOSR J. **5**, 2320–7388 (2015)
16. T. Hurma, S. Kose, XRD Raman analysis and optical properties of CuS nanostructured film. Optik **127**(15), 6000–6006 (2016)
17. S. Yadav, K. Shrivas, P.K. Bajpai, Role of precursors in controlling the size, shape and morphology in the synthesis of copper sulfide nanoparticles and their application for fluorescence detection. J. Alloy. Compd. **772**, 579–592 (2019)
18. T. Thongtem, A. Phuruangrat, S. Thongtem, Characterization of copper sulfide nanostructured spheres and nanotubes synthesized by microwave-assisted solvothermal method. Mater. Lett. **64**(2), 136–139 (2010)
19. M. Placidi, M. Dimitrievska, V. Izquierdo-Roca, X. Fontané, A. Castellanos-Gomez, A. Pérez-Tomás, V. Bermudez, Multiwavelength excitation Raman scattering analysis of bulk and two-dimensional MoS2 vibrational properties of atomically thin MoS2 layers. 2D Mater. **2**(3), 035006 (2015)
20. J. Zou, J. Zhang, B. Zhang, P. Zhao, X. Xu, J. Chen, K. Huang, Synthesis and characterization of copper sulfide nanocrystal with three-dimensional flower-shape. J. Mater. Sci. **42**(22), 9181–9186 (2007)
21. H. Shimose, M. Singh, D. Ahuja, W. Zhao, S. Shan, S. Nishino, J. Luo, Copper Sulfide-Zinc Sulfide Janus nanoparticles and their Seebeck characteristics for sustainable thermoelectric materials. J. Phys. Chem. C **120**(11), 5869–5875 (2016)
22. S. Ikram, J. Jacob, K. Mehboob, K. Mahmood, A. Ashfaq, A. Ali, U. Rehman, A novel approach to simultaneously enhance the Seebeck coefficient and electrical conductivity in rutile phase of TiO2 nanostructures. Arab. J. Chem. **13**(8), 6724–6729 (2020)
23. A. Ashfaq, J. Jacon, A. Ali, K. Mehboob, K. Mahmood, U. Rehman, M.I. Arshad, Designing of Seebeck coefficient and electrical conductivity in CZTS thin films for giant power factor. Ceram. Int. **46**(7), 9646–9655 (2020)

Publisher's Note Springer Nature remains neutral with regard to jurisdictional claims in published maps and institutional affiliations.